

# Rheological behavior of compatibilized and non-compatibilized PA6/EPM blends

Jorge Silva · Ana Vera Machado · João Maia

Received: 8 June 2006 / Accepted: 26 April 2007 / Published online: 20 May 2007  
© Springer-Verlag 2007

**Abstract** The rheological properties of PA-6/EPM polymer blends, non-compatibilized and compatibilized with grafted ethylene propylene rubber (EPM-g-MA), have been investigated. Linear and non-linear (relaxation both in shear and extension) experiments were realized. Stress relaxation experiments coupled with scanning electron microscopy (SEM) analysis showed the existence of one relaxation time and non-deformed droplets for the immiscible blend, and two relaxation times and deformed droplets for the compatibilized ones, the second relaxation being more pronounced for higher compatibilizer contents. These results clearly indicate that, despite the high viscosity and elasticity ratios, if high amounts of compatibilizer are added to the blend, interfacial slip is suppressed and a high-enough adhesion between the phases is achieved for the high-viscosity dispersed phase to be deformed.

**Keywords** Polymer blends · Compatibilization · Interface · Nonlinear rheology · PA-6/EPM blends · Droplet deformation

## Introduction

Blending polymers is a relatively cheap way to generate high performance materials. Blends already represent a large fraction of all plastics produced. Their properties depend strongly on the properties of the components and on

the morphology, as most of polymer blends of industrial interest are generally immiscible. However, the behavior of interfaces during polymer blend processing is not well understood yet and is the subject of much ongoing research worldwide.

The first model to predict with relative accuracy the dynamic modulus of a two-phase system with viscoelastic components was proposed by Palierne (1990). Although it is only valid for small-amplitude oscillatory flow, it has been shown to be in good agreement with experimental data (e.g., Graebling et al. 1993). To predict the dynamic moduli of the blend using this model, it is necessary to know the dynamic moduli of the matrix and dispersed phase, the interfacial tension, and the size distribution of the droplets. In the Palierne model, the distribution of droplet radius can be substituted by the volumetric mean radius, provided that the polydispersity index ( $R_v/R_n$ ) does not exceed the value of 2 (Graebling et al. 1993).

In terms of the response to extensional flows, Delaby et al. (1994, 1995, 1996a, 1996b) studied blends with well-controlled number and size of droplets and viscosity ratios. The authors found that the droplet deforms less than the macroscopic deformation of the sample when it is more viscous than the matrix and more than the matrix (approximately 5:3 times) when it is less viscous, which is in accordance with the theories of Taylor (1934) and Cox (1969) for vanishing interfacial tension. Delaby et al. (1994, 1995, 1996a, 1996b) also used Palierne's linear model to derive a first-order time evolution deformation of the droplet during start-up of flow. Mighri et al. (1997) used a convergent die to generate an apparent elongation flow and showed that the droplet deformation is not only governed by the viscosity ratio but also by the elasticity ratio, defined as the ratio between the relaxation time of the dispersed phase to that of the matrix. They observed that the droplet deformation increases with

---

Paper presented at the 3rd Annual European Rheology Conference, April 27–29, 2006, Crete, Greece

---

J. Silva · A. V. Machado · J. Maia (✉)  
Department of Polymer Engineering, IPC—Institute for Polymers and Composites, University of Minho,  
4800-058 Guimarães, Portugal  
e-mail: jmaia@dep.uminho.pt

increasing elasticity of the matrix and decreases with increasing elasticity of the droplet. The elongational properties of acrylonitrile–butadiene–styrene (ABS) polymer melts were investigated by Takahashi et al. (1997) who showed that strain-hardening could be correlated with the deformability of the butadiene particles. The strain hardening of the samples containing hard butadiene particles was strongly reduced in comparison with soft ones because of a length decrease of the region of elongational flow. Oosterlinck et al. (2005), while studying poly(methyl methacrylate)-polystyrene (PMMA-PS) blends subjected to uniaxial elongation flows, verified that the extra stress due to droplet deformation can, in principle, be deduced from extensional rheological measurements. However, experimental studies about the morphological development of immiscible blends during uniaxial elongational flows are rare, and some aspects, mainly those concerned with the influence of elasticity, need to be clarified.

The elongation and subsequent recovery of PS/PMMA blends, as well as the evolution of morphology, were studied by Gramespacher and Meissner (1997) and, more recently, by Mechbal and Bousmina (2004) and Handge and Pötschke (2004). Pronounced differences were observed in the recovery behavior after melt elongation, that of the blends being much larger than that of the blend components. The results suggest that, in polymer blends, there is a fast molecular recovery related with each component and a slow one associated with interfacial tension.

Over the last years, the use of compatibilizers has become a usual practice because the compatibilizers enhance adhesion between the two phases and stabilize the morphology, leading to a finer morphology. Compatibilization can be achieved by different methods, such as the addition of a pre-synthesized copolymer or creating in situ, during the blending process, a third component, often called an interfacial agent, emulsifier, or compatibilizer (Utracki 1994; Datta and Lohse 1996a, b). This component can be a graft or block copolymer, which tends to be located at the interfaces between the two components of the blend.

The first method, *ex situ*, has the advantage of better control of the molecular architecture of the compatibilizer. However, it requires specific chemical routes and reaction conditions. In the second method, also called reactive blending or *in situ* compatibilization, the generation of the compatibilizer is performed in situ at the interfaces directly during blending. To generate the copolymer at the interface, both polymers must have reactive groups. For example, the terminal amine groups of PA-6 can react with maleic anhydride groups of the modified polyolefins. Moreover, because the compatibilizer is formed in situ at the interfaces, the problem of getting it there no longer exists. For these reasons, this second method has become very attractive recently. Nevertheless, because the reaction takes

place primarily in the interfaces, it is difficult to control the rate of formation, the amount, and the molecular architecture of the compatibilizer.

In addition, the behavior of the interfaces modified by compatibilizers is not well understood yet. Most of the rheological studies in this area deal with the blends compatibilized with a pre-synthesized block copolymers (Van Puyvelde et al. 2001), revealing a new relaxation process in this type of blends. For example, Riemann et al. (1997) showed that the addition of P(S-*b*-MMA) and P(CHMA-*b*-MMA) block copolymers at PS/PMMA blends originates a new relaxation time,  $\tau_{\beta}$ . Moreover, they observed that the addition of a compatibilizer causes a slight increasing of the shape relaxation time,  $\tau_1$ . Considering non-isotropic interfacial stress in the Palierne model, the authors predicted the relaxation time  $\tau_{\beta}$ . In fact, some studies (Van Hemelrijck et al. 2004) suggest that the concentration of compatibilizer can change along the droplet interface, leading to an extra stress called the Maragoni stress.

It has been reported that the presence of compatibilizers suppresses droplet coalescence (Van Puyvelde et al. 2001; Van Hemelrijck et al. 2004) and reduces or eliminates interfacial slip. For example, Van Puyvelde et al. (2003), studying PA-6/EPR blends, had observed a negative deviation from the log-additivity rule. They observed that the addition of compatibilizer suppresses slip, significantly increasing the viscosity of the blend. Their studies support the hypothesis that the interfacial slip is due to loss of entanglements in the interfacial region.

The scaling laws of Doi and Ohta (1991) on the shear stress were verified experimentally by Iza et al. (2001) for PS/HDPE blends physically compatibilized with copolymers. However, these authors verified that  $N_1$  does not scale with  $\dot{\gamma}$  but with  $\dot{\gamma}^{\alpha}$ , where  $\alpha$  is close to 2. Moreover, it was demonstrated that the amount of compatibilizer, as well as its structure, drastically affects the rheological response to a sudden imposition of a shear rate.

Macaúbas et al. (2005), using blends of PP/PS compatibilized with a linear triblock copolymer (styrene–ethylene–butylene–styrene, SEBS), observed that the scaling laws are not valid for the shear stress. They formulated a model using the ideas of Doi and Ohta (1991), Lacroix et al. (1998), and Bousmina et al. (2001) that was able to predict the behavior of non-compatibilized blends for a single step shear. However, the model does not predict the behavior of compatibilized blends. Finally, Silva et al. (2006) observed that the shear behavior of PA-6/EPM blends is altered by *in situ* compatibilization. They observed that the addition of EPM-*g*-MA compatibilizer leads to an increase of dynamic moduli, mainly at low frequencies, and to the appearance of a second longer relaxation time in shear.

From the above review, it results quite clear that the rheological behavior of blends (compatibilized and non-

compatibilized) with high viscosity and elasticity ratios is not well understood yet despite their obvious industrial importance. Thus, the main aim of the present work is to understand the role of the in situ compatibilization of these materials, namely, to assess whether the high viscosity, high elasticity droplets of the dispersed phase are viscoelastically deformed under flow, and what the implications in the overall rheological behavior of the materials are.

## Experimental

### Materials

Several blends of a commercial polyamide-6 (PA-6 Akulon K123), an ethene–propene rubber (EPM Keltan 740) and an ethene–propene rubber modified with maleic anhydride (EPM-g-MA ExxelorVA 1801, containing 0.49 wt% of MA, as determined by Fourier transform infrared (FTIR), were prepared in a twin-screw extruder under the same process conditions. The PA-6 content was kept constant in all blends, but the amount of modified rubber was varied to have different amounts of maleic anhydride in each blend and, thus, various amounts of compatibilizer at the interface. The chemical and morphological characterizations were performed in a previous work (Machado et al. 1999), some data being summarized in Tables 1 and 2. The volume ( $R_v$ ) and number ( $R_n$ ) average radii were calculated using Eqs. 1 and 2:

$$R_v = \frac{\sum_i n_i R_i^4}{\sum_i n_i R_i^3} \quad (1)$$

$$R_n = \frac{\sum_i n_i R_i}{\sum_i n_i} \quad (2)$$

where  $n_i$ =number of the droplets having radius  $R_i$ .

**Table 1** Compounding of the blends

Blend (w/w/w)	PA6 (wt%)	EPM (wt%)	EPM-g-MA (wt%) <sup>a</sup>	MA content of rubber phase (wt%) <sup>b</sup>
80:20:0	80	20	0	0
80:15:5	80	15	5	0.13
80:10:10	80	10	10	0.25
80:5:15	80	5	15	0.37
80:0:20	80	0	20	0.49

<sup>a</sup>MA content of EPM-g-MA is 0.49 wt%.

<sup>b</sup>MA content of the rubber phase is the weight average of the combined EPM and EPM-g-MA rubber phases.

**Table 2** Morphological characterization of the blends

Blend (w/w/w)	$R_v$ ( $\mu\text{m}$ )	$R_n$ ( $\mu\text{m}$ )	$R_v/R_n$
80:20:0	17.6	5.6	3.1
80:15:5	8.25	1.28	6.5
80:10:10	2.35	1.18	2.0
80:5:15	1.78	1.11	1.6
80:0:20	0.36	0.20	1.8

### Shear rheometry

The rheological measurements in shear were performed in a Reologica Stress Tech HR rheometer, using a parallel plate geometry (diameter=25 mm) with a  $1,000 \pm 1 \mu\text{m}$  gap. Samples were vacuum dried at 80 °C during 12 h before each rheological experiment.

All oscillatory tests were performed at three different temperatures (240, 260, 280 °C) in a nitrogen atmosphere, time sweep measurements at constant frequency having been performed to ensure that neither polymerization nor degradation occurred during the frequency sweep tests (Figs. 1 and 2).

The stress relaxation experiments were performed at 240 °C in a nitrogen atmosphere; a shear rate of  $0.1 \text{ s}^{-1}$  during 250 s was applied, and the shear stress upon cessation of flow was measured. Because it is likely that the processing of blends causes degradation (by chain scission/crosslinking) of the polyamide to have comparable results for the PA6 and the blends, the former was also extruded under the same conditions as the latter. Thus, all the results shown below are not for virgin PA6, but for extruded PA6.

### Extensional rheometry

The extensional rheological measurements were performed on the modified rotational rheometer (MRR) developed by Maia et al. (1999). For start-up extensional measurements, extruded samples (either in a Leistritz twin-screw extruder blends or in a Rosand RH8-2 capillary rheometer–EPM and EPM-g-MA) were used. For extensional relaxation experiments, samples with rectangular cross-section (about  $3 \times 2 \text{ mm}$ ) necessary to increase the signal were prepared by compression molding. All the samples were vacuum dried at 80 °C during 12 h before the corresponding rheological experiments.

Upon loading onto the rheometer, residual stresses were allowed to relax; once the measured torque decayed to zero, any existing slack was removed, which was followed by another waiting period for residual stress relaxation; only once the measured torque decayed to zero again would the experiment be started. The effective length of each sample

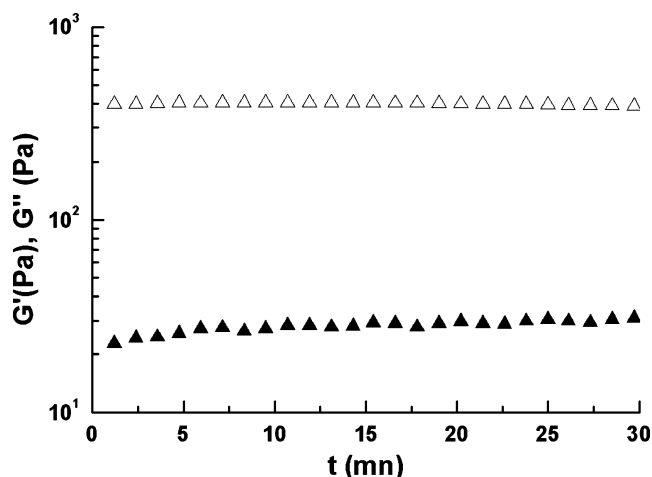


**Fig. 1** Dynamic moduli of PA6 measured at a constant frequency (0.1 Hz) at 260 °C in a nitrogen atmosphere

was 40 mm, and the diameter varied between 2 and 3 mm, thus, yielding an aspect ratio,  $L/D$ , ranging between approximately 13 and 20, which has been shown (Barroso et al. 2002) to be high enough for end effects to be negligible. During all the experiments, the samples were immersed in silicone oil at 240 °C for the dual purpose of temperature control and sagging prevention. The particular details on the experimental technique to measure the stress relaxation after an extensional step strain are given in Barroso and Maia (2002).

The main motivation for performing extensional rheometry experiments on these samples is related to the fact that their viscosity and elasticity ratios are very high (see below) and, therefore, any differences in rheological behavior, especially due to interfacial phenomena, between the immiscible and the compatibilized blends are likely to be better seen in extensional flows than is shear (e.g., Oosterlinck et al. 2005).

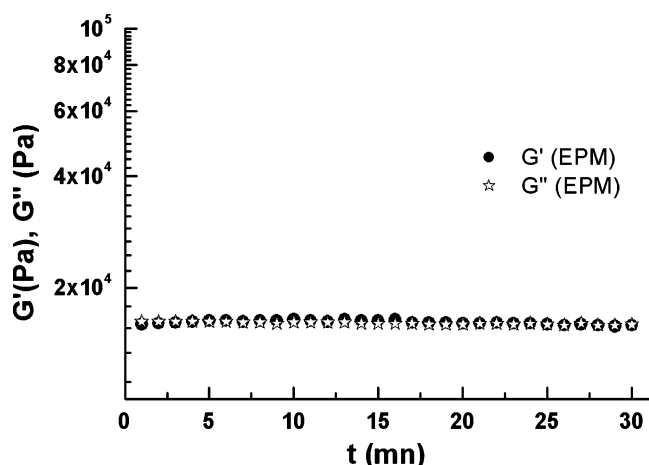


**Fig. 2** Dynamic moduli of EPM measured at a constant frequency (0.1 Hz) at 240 °C

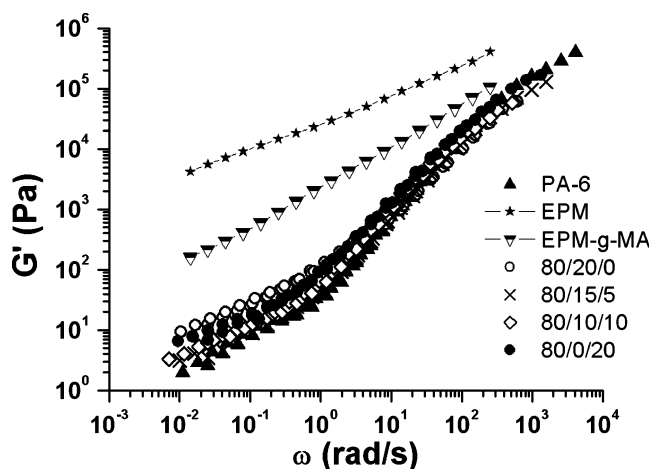


**Fig. 3** Storage modulus for several blends of PA6/EPM/EPM-g-MA and their components

### Morphology

To study the morphology of samples undergoing extensional deformations, the oil bath was rapidly removed during an experiment and the deformed sample was quenched in liquid nitrogen (the whole process takes only 2 to 3 s) while the deformation is still being imposed. This means that no significant morphological changes, such as droplet relaxation and/or coalescence, should occur during the quenching process. Once solidified, the samples were fractured longitudinally in liquid nitrogen, etched with boiling xylene to remove the rubber from the surface and gold plated; their morphology was studied using a Jeol JSM 6310F scanning electron microscope.

### Results and discussion

Figures 3 and 4 show the dynamic moduli of the blends and their components (PA-6, EPM, EPM-g-MA). Time-temperature superposition was performed at a reference temperature of 260 °C for PA-6 and the blends. From the figures, it is possible to observe that the  $t-T$  superposition works well at high frequencies, while at low frequencies, there is some scatter in the data, and it is possible that, especially at the higher temperatures, sample degradation is starting to set in. However, because the experiments were performed in a nitrogen atmosphere, this is not very likely; in addition, because the scatter is not large enough to mask the qualitative behavior of the  $G'$  and  $G''$  curves, the option was made to keep the data.

The figures show that the blends have different qualitative behaviors depending on the amount of compatibilizer. At high frequencies, all the blends except the one with the highest compatibilizer content show an effect commonly known as negative deviation behavior, NDB, which origi-

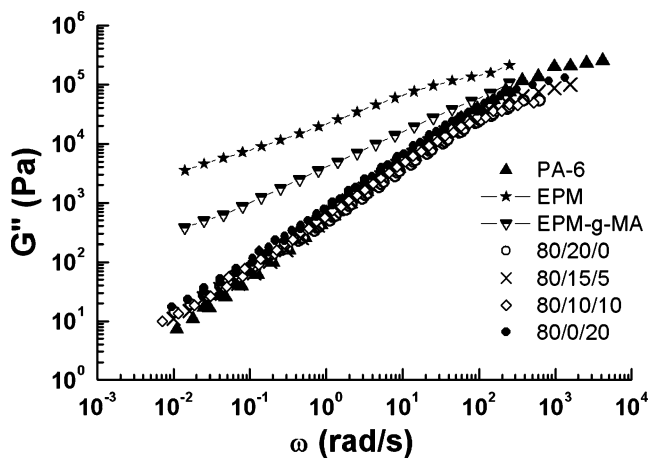


**Fig. 4** Dissipative modulus for several blends of PA6/EPM/EPM-g-MA and their components

nates in slip at the interfaces (Utracki 1983; Van Puyvelde et al. 2003) due to poor or insufficient compatibilization between the matrix and the dispersed phase. At low frequencies, an increase in the moduli of the blends can be noticed. This is especially noticeable at very low frequencies where a plateau in  $G'$ , which has been related to the size of the particles of the dispersed phase and the amount of compatibilizer at the interfaces (Riemann et al. 1997; Van Hemelrijck et al. 2004), seems to develop.

Again, it could be argued that this plateau could also be attributed to changes in rheological properties of the components during the experiment, e.g., degradation. However, as shown in Figs. 1 and 2, the rheological behavior of PA-6 and EPM remains very much constant in time at the time-scale of the experiments.

Because the viscosity ratios are very high (approximately 50 and 400 between PA6 and EPM, at  $3 \times 10^{-3}$  Hz), the Palierne model is not able to predict, even qualitatively, these results.

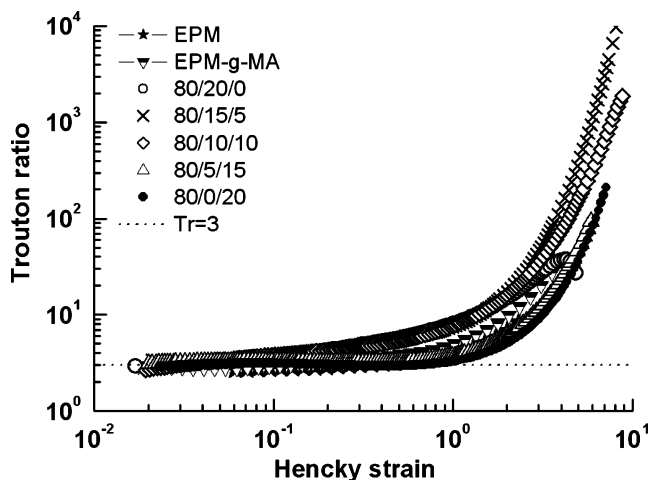


**Fig. 5** Trouton ratios for all blends. Strain rates,  $\dot{\epsilon}$ : 80/20/0,  $0.10 \text{ s}^{-1}$ ; 80/15/5,  $0.11 \text{ s}^{-1}$ ; 80/10/10,  $0.16 \text{ s}^{-1}$ ; 80/5/15,  $0.14 \text{ s}^{-1}$ ; 80/0/20,  $0.13 \text{ s}^{-1}$ ; EPM,  $0.10 \text{ s}^{-1}$ ; EPM-g-MA,  $0.11 \text{ s}^{-1}$

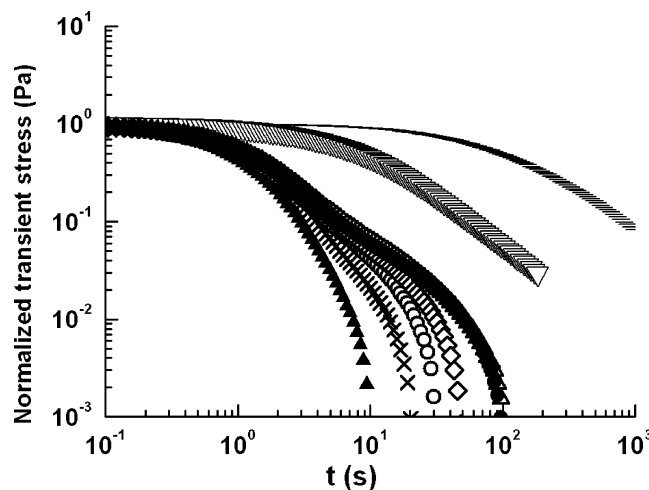


**Fig. 6** Normalized transient stress for several blends of PA6/EPM/EPM-g-MA and their components after cessation of a shear flow of  $0.1 \text{ s}^{-1}$ . Filled triangle PA-6, bar EPM, inverted open triangle EPM-g-MA, open circle 80/20/0, cross 80/15/5, diamond 80/10/10, open triangle 80/5/15, filled circle 80/0/20

Figure 5 shows the transient Trouton ratios for all the materials in uniaxial extension (except PA6 that was not possible to test due to its low viscosity), the main features being:

- (a) All the materials show a pronounced strain hardening due to the existence of a rubber phase. In the non-compatible blend, the degree of strain hardening is much smaller than in the remainder, which is a further indication of poor adhesion between the two phases.
- (b) The onset of strain hardening is much lower (of the order  $\epsilon_H=0.1$ ) for the non-compatible and the insufficiently compatibilized blends (EPM-g-MA content equal or lower than 10%) than for those with higher MA contents (of the order  $\epsilon_H=1$ ).

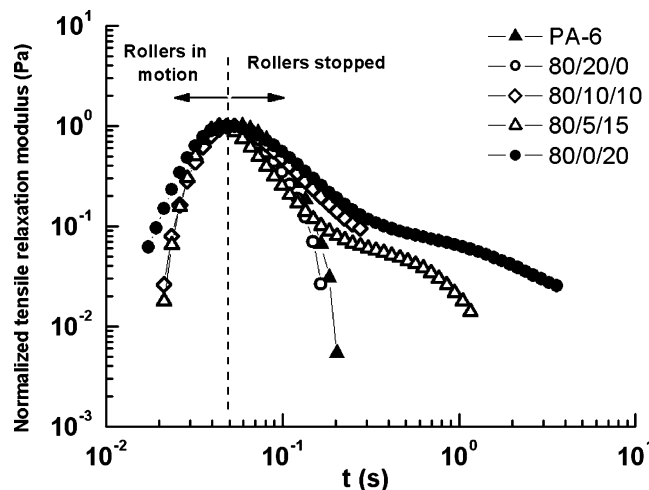
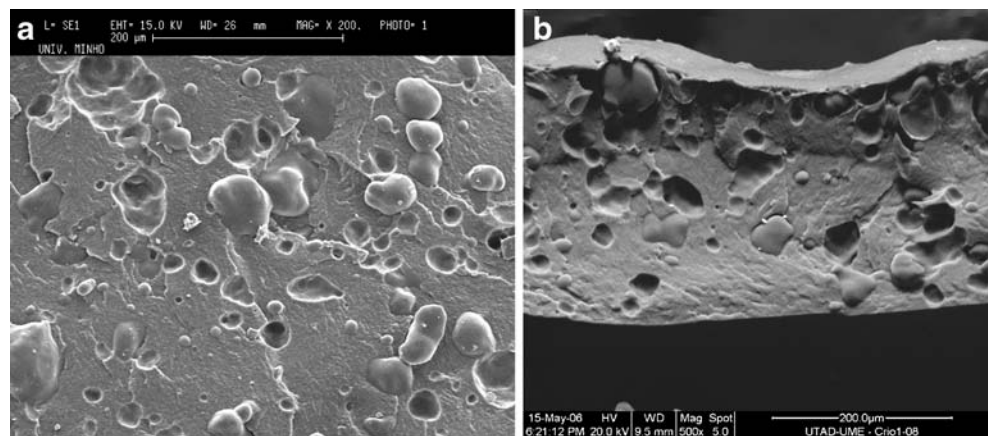


**Fig. 7** Normalized relaxation modulus flow for the blends and their components. Strain rates are PA-6,  $15.6 \text{ s}^{-1}$ ; 80/20/0,  $0.98 \text{ s}^{-1}$ ; 80/10/10,  $0.98 \text{ s}^{-1}$ ; 80/5/15,  $0.24 \text{ s}^{-1}$ ; 80/0/20,  $0.54 \text{ s}^{-1}$

**Fig. 8** SEM micrographs of the fracture surfaces of the 80/20/0 blend: **a** non-deformed sample and **b** after extension (the sample was stretched during 5 s at a strain rate of  $0.08 \text{ s}^{-1}$ )



Again, this is presumably due to the better adhesion between the phases; i.e., the presence of the rubber stabilizes the blend and increases the range of linear viscoelastic response (note that the onset of strain hardening for the EPM and EPM-g-MA are very similar to those of the 15 and 20% EPM-g-MA blends).

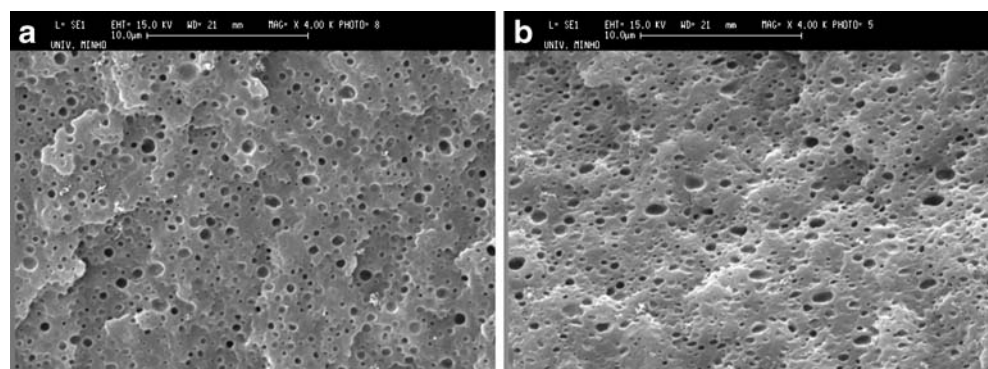
Shear stress relaxation measurements (Fig. 6) illustrated that all blends relax in two consecutive steps. The first (faster) step should be related with the relaxation of the PA-6 matrix, and the second (slower) step is probably due to relaxation of EPM and/or interfaces. In this case, particle size and interfacial adhesion play a determinant role in the shear stress relaxation function. For the compatibilized blends, the second relaxation time increases in duration with increasing amount of compatibilizer up to a EPM-g-MA content of 15%, which indicates that the effect is related with a better adhesion at the interfaces and saturates at 15% EPM-g-MA concentration. An interesting feature in Fig. 6 is that the second relaxation time of the 80/15/5 blend is slightly shorter than the one of the non-compatibilized blend, which indicates that low compatibilizer amounts are enough to decrease significantly the droplets' average size but not to prevent the slip between the phases.

As in the shear relaxation experiments, in the extensional relaxation (after a step strain) experiments, the compatibilized blends exhibits higher relaxation times (Fig. 7). Once

more, the fast relaxation time can be attributed to the PA-6 matrix and the slow one to the interface and/or rubber dispersed phase. This suggests that the presence of slip at the interface inhibits the deformation of dispersed phase droplets and that this effect is corrected with the addition of EPM-g-MA. However, this needs to be confirmed by a morphological analysis of stretched samples on a SEM.

Representative results of the morphological analysis are depicted in Figs. 8 and 9 for the non-compatibilized and the highest compatibilizer content blends, respectively. Figure 8 shows the morphologies of the non-compatibilized blend (a) before extension and (b) quenched during extension, and the similarities are immediately apparent: in both cases, droplets are essentially spherical. Thus, there was no (or only negligible) deformation of the rubber phase upon extension due to interfacial slip. In the compatibilized blend, the average droplet size is much smaller, as would be expected, and the morphologies before (Fig. 9a) and after (Fig. 9b) extension are quite different. In the former case, the expected spherical droplet morphology is seen, and in the latter, the droplets are very elongated, but still quite large. This is an indication that the compatibilizer was present in an enough content to make the drag force on the droplets overcome the resistance to flow/deformation of the rubber phase (note that the viscosity ratio is very high in these materials).

**Fig. 9** SEM micrographs of the fracture surfaces of the 80/0/20 blend: **a** non-deformed sample and **b** after extension (the sample was stretched during 5 s at a strain rate of  $0.08 \text{ s}^{-1}$ )



## Conclusions

In the present work, the rheological proprieties of immiscible and compatibilized blends with high viscosity and elasticity ratios were studied. Despite this fact, the rubber droplets do not exhibit a rigid sphere-like behavior. In fact, oscillatory shear, uniaxial extension, and stress relaxation experiments (in both shear and extension) showed the existence of one relaxation time for the immiscible blend and two for the compatibilized ones that, in all cases, is more pronounced for higher compatibilizer contents. Together with SEM evidence of the existence of elongated droplets after extension for the compatibilized blends and spherical ones in the non-compatibilized ones, these results clearly indicate that, despite the high viscosity and elasticity ratios, if high enough amounts of compatibilizer are added to the blend, interfacial slip is suppressed and a high-enough adhesion between the phases is achieved for the high-viscosity dispersed phase to be deformed.

**Acknowledgment** The authors would like to thank to the Foundation for Science and Technology–FCT for awarding one of them (Jorge Silva) a PhD Fellowship (ref. BD/12833/2003) within the framework of Programa Operacional “Ciência, Tecnologia, Inovação” (POCTI) and Programa Operacional Sociedade da Informação (POSI) of the Quadro Comunitário de Apoio III (2000–2006).

## References

- Barroso VC, Maia JM (2002) Evaluation by means of stress relaxation (after a step strain) experiments of the viscoelastic behavior of polymer melts in uniaxial extension. *Rheol Acta* 41:257–264
- Barroso VC, Covas JA, Maia JM (2002) Sources of error and other difficulties in extensional rheometry revisited: commenting and complementing a recent paper by T. Schweizer. *Rheol Acta* 41: 154–161
- Bousmina M, Aouina M, Chaudhry B, Guenette R, Bretas RES (2001) Rheology of polymer blends: non-linear model for viscoelastic emulsions undergoing high deformation flows. *Rheol Acta* 40:538–551
- Cox RG (1969) Deformation of a drop in a general time-dependent fluid flow. *J Fluid Mech* 37:601–623
- Datta S, Lohse D (1996) Polymeric compatibilizers. Hanser, Munich
- Datta S, Lohse D (1996) Polymeric compatibilizers, uses and benefits in polymer blends. Hanser, Munich
- Delaby I, Ernst B, Germain Y, Muller R (1994) Droplet deformation in polymer blends during uniaxial elongational flow-influence of viscosity ratio for large capillary numbers. *J Rheol* 38:1705–1720
- Delaby I, Ernst B, Muller R (1995) Drop deformation during elongational flow in blends of viscoelastic fluids. Small deformation theory and comparison with experimental results. *Rheol Acta* 34:525–533
- Delaby I, Ernst B, Muller R (1996a) Drop deformation in polymer blends during elongational flow. *J Macromol Sci Phys* B35:547–561
- Delaby I, Ernst B, Froelich D, Muller R (1996b) Droplet deformation in immiscible polymer blends during transient uniaxial elongational flow. *Polym Eng Sci* 36:1627–1635
- Doi M, Ohta T (1991) Dynamics and rheology of complex interfaces, I. *J Chem Phys* 95:1242–1248
- Graebing D, Muller R, Palierne JF (1993) Linear viscoelastic behavior of some incompatible polymer blends in the melt-interpretation of data with a model of emulsion of viscoelastic liquids. *Macromolecules* 26:320–329
- Gramespacher H, Meissner J (1997) Melt elongation and recovery of polymer blends, morphology, and influence of interfacial tension. *J Rheol* 41:27–44
- Handge UA, Potschke P (2004) Interplay of rheology and morphology in melt elongation and subsequent recovery of polystyrene/poly (methyl methacrylate) blends. *J Rheol* 48:1103–1122
- Iza M, Bousmina M, Jerome R (2001) Rheology of compatibilized immiscible viscoelastic polymer blends. *Rheol Acta* 40:10–22
- Lacroix C, Grmela M, Carreau PJ (1998) Relationships between rheology and morphology for immiscible molten blends of polypropylene and ethylene copolymers under shear flow. *J Rheol* 42:41–62
- Macaubas PHP, Demarquette NR, Dealy JM (2005) Nonlinear viscoelasticity of PP/PS/SEBS blends. *Rheol Acta* 44:295–312
- Machado AV, Covas JA, Van Duin M (1999) Chemical and morphological evolution of PA-6/Epm/Epm-g-MA blends in a twin screw extruder. *J Polym Sci Polym Chem* 37:1311–1320
- Maia JM, Covas JA, Nobrega JM, Dias TF, Alves FE (1999) Measuring uniaxial extensional viscosity using a modified rotational rheometer. *J Non-Newton Fluid Mech* 80:183–197
- Mechbal N, Bousmina M (2004) Uniaxial deformation and relaxation of polymer blends: relationship between flow and morphology development. *Rheol Acta* 43:119–126
- Mighri F, Ajji A, Carreau PJ (1997) Influence of elastic properties on drop deformation in elongational flow. *J Rheol* 41: 1183–1201
- Oosterlinck F, Mours M, Laun HM, Moldenaers P (2005) Morphology development of a polystyrene/polymethylmethacrylate blend during start-up of uniaxial elongational flow. *J Rheol* 49:897–918
- Palierne JF (1990) Linear rheology of viscoelastic emulsions with interfacial-tension. *Rheol Acta* 29:204–214
- Riemann RE, Cantow HJ, Friedrich C (1997) Interpretation of a new interface-governed relaxation process in compatibilized polymer blends. *Macromolecules* 30:5476–5484
- Silva JM, Machado AV, Maia JM (2006) Transient rheological behaviour of PA6/EPM/EPM-g-MA blends. *Adv Mater Forum* III 514–516:853–857
- Takahashi T, Wu WG, Toda H, Takimoto J, Akatsuka T, Koyama K (1997) Elongational viscosity of ABS polymer melts with soft or hard butadiene particles. *J Non-Newton Fluid Mech* 68:259–269
- Taylor GI (1934) The formation of emulsions in definable fluids of flow. *Proc R Soc A* 146:501–523
- Utracki LA (1983) Melt flow of polymer blends. *Polym Eng Sci* 23: 602–609
- Utracki LA (1994) Encyclopaedic dictionary of commercial polymer blends. ChemTec, Toronto
- Van Hemelrijck E, Van Puyvelde P, Velankar S, Macosko CW, Moldenaers P (2004) Interfacial elasticity and coalescence suppression in compatibilized polymer blends. *J Rheol* 48:143–158
- Van Puyvelde P, Velankar S, Moldenaers P (2001) Rheology and morphology of compatibilized polymer blends. *Curr Opin Colloid Interface Sci* 6:457–463
- Van Puyvelde P, Oommen Z, Koets P, Groeninckx G, Moldenaers P (2003) Effect of reactive compatibilization on the interfacial slip in nylon-6/EPR blends. *Polym Eng Sci* 43:71–77